Atypically larger variability of resource allocation accounts for visual working memory deficits in schizophrenia

Running title: visual working memory in schizophrenia

Yi-Jie Zhao[1], Tianye Ma[1], Xuemei Ran[1], Li Zhang[1], Ru-Yuan Zhang[2*], Yixuan Ku[1*]

[1]The Shanghai Key Lab of Brain Functional Genomics, Shanghai Changning-ECNU Mental Health Center, School of Psychology and Cognitive Science, East China Normal University, Shanghai, 200062 China

[2]Center for Magnetic Resonance Research, Department of Neuroscience, University of Minnesota, Minneapolis, MN 55455 USA

* co-corresponding author

Correspondence:

Yixuan Ku: yxku@psy.ecnu.edu.cn

Ru-Yuan Zhang: zhan1217@umn.edu

Abstract

Schizophrenia patients are known to have profound deficits in visual working memory (VWM), and almost all previous studies attribute the deficits to decreased memory capacity. This account, however, ignores the potential contributions of other VWM components (e.g., memory precision). Here, we measure the VWM performance of 60 schizophrenia and 61 healthy control subjects. Moreover, we thoroughly evaluate several established computational models of VWM to compare the performance of the two groups. Surprisingly, none of the models reveal group differences in memory capacity and memory resources. We find that the model assuming variable precision across items and trials is the best model to explain the performance of both groups. According to the variable-precision model, schizophrenia subjects exhibit abnormally larger variability of allocating memory resources rather than resources or capacity per se. These results challenge the widely accepted decreased-capacity theory and propose a new perspective on the diagnosis and rehabilitation of schizophrenia.

Keywords: Schizophrenia, Visual working memory, Memory precision, Memory capacity, Bayesian inference, Perceptual variability

Introduction

Schizophrenia is a severe mental disorder accompanied by a range of dysfunctions in perceptual and cognitive behavior, among which working memory deficit is considered as a core feature [1–4]. Working memory refers to the ability to temporally store and manipulate information in order to guide appropriate behavior, and it has been shown to link with a broad range of other brain functions, including perception, attention, problem-solving and executive control [5–8]. Dysfunctions in working memory therefore might cascade into multiple mental processes, causing a wide spectrum of negative consequences [2,3,9].

A well-established finding in lab-based experiments is that people with schizophrenia (SZ) exhibit worse performance than healthy control (HC) in visual working memory (VWM) tasks [2]. This phenomenon has long been attributed to decreased VWM capacity in SZ [2,10,11]. This theory was supported by previous studies using various VWM or other WM tasks, including the 'span' tasks (e.g., digit span, spatial span, verbal span) [12,13], the N-back task [14–16], the delayed-response task [17–19], the change detection task [20–24], and the delay-estimation task [25–27]. Despite the considerable differences across tasks, almost all previous studies converged to the same conclusion that decreased-capacity is the major cause of the VWM deficits in SZ.

Besides capacity, in the basic research of VWM, people have increasingly recognized memory *precision* as another pivotal determinant of VWM performance [28]. Precision reflects the amount of memory resources assigned to individual items—a larger amount of resources leads to higher memory precision. At the neural level, low perceptual precision might arise from either the intrinsic noise in neural processing [29–31] or the fluctuations of cognitive factors (e.g., arousal, attention) [31,32]. Atypically increased variability in both behavioral and neural responses has been discovered in patients with mental diseases such as autism spectrum disorder [33,34], dyslexia [35], and attention-deficit/hyperactivity disorder [36]. These theoretical and empirical studies raise the possibility that SZ and HC might differ in memory precision rather than capacity— that is, these two groups might be able to remember an equal number of items (i.e., comparable capacity) but SZ generally process and maintain items in a less precise manner. Only a few studies have attempted to simultaneously quantify memory capacity and precision in schizophrenic or schizotypy subjects, and the results are not consensus [25,26].

Despite the confound of the possible cause in different VWM components, it is unclear whether SZ and HC employ the same computational strategies (i.e., observer model) in VWM. Most prior studies only used one model and implicitly assumed the model was the best one for both SZ and HC. But without systematic model comparisons model optimality cannot be firmly warranted, and endowed results might be biased by the choice of a particular model. Given that several influential models have been proposed to explain the VWM behavior in normal subjects [28], it remains unclear which one is the best for SZ. If the best model for SZ differs from the one for HC, it indicates that the two groups use qualitatively different computational strategies to complete behavioral tasks. If SZ and HC share the same best model, it indicates that they use the same strategy but quantitatively different parameters. These possibilities, however, have yet been thoroughly tested.

In the present study, we aim to systematically disentangle the impact of memory capacity and precision, as well as other factors (i.e., variability in allocating resources and variability in choice) in SZ. In this study, the performance of SZ and demographically matched HC was measured in a standard VWM delayed-estimation task (Fig. 1). Using a standard task allows us to compare our results to that from previous studies [25,37–40]. Most importantly, in contrast to most prior studies, we evaluated and compared almost all mainstream computational models in visual working memory research. This approach allows us to take an unbiased perspective and search a large space of both models and parameters. We believe that a well-controlled task and thorough computational modeling will shed new light on the mechanisms of VWM deficits associated with schizophrenia.

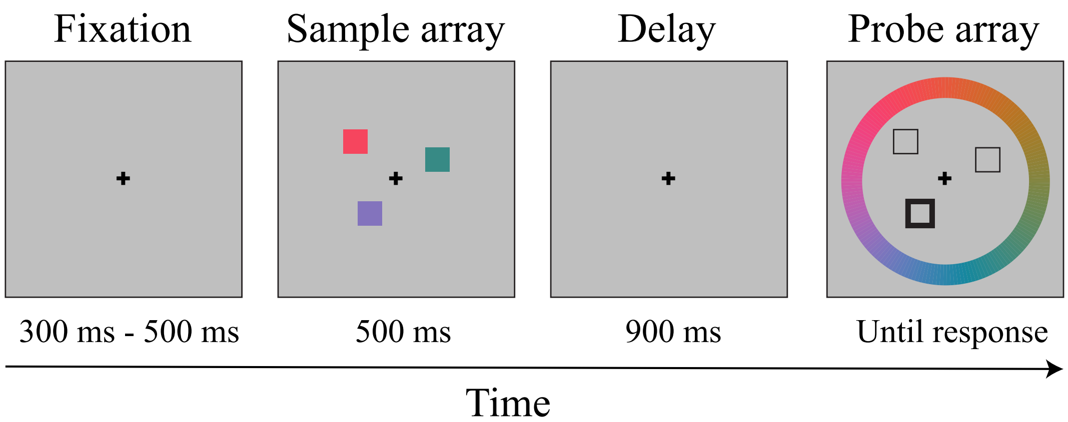

Figure 1. Color delay-estimation task. This figure depicts an example trial (i.e., set size = 3) of the color delay-estimation task. Subjects are instructed to first memorize the colors of all squares on the screen, and after a 900ms delay choose the color of the probed square (the one in the left lower visual field in this example) on a color wheel. Response error is the difference between the reported color and the real color of the probe in the standard color space.

Results

Worse VWM performance in SZ

We first look at the histograms of raw response errors (the circular distance between the original color and the chosen color, Fig. 2A). The circular standard deviation (CSD) of the response errors was calculated to indicate VWM performance. A repeated-measure ANOVA was performed with CSD as the dependent variable, set size (1/3) as the within-subject variable, group as the between-subject variable (Fig. 2B). As demonstrated by previous studies, VWM performance was worse when set size was higher ($F(1,119) = 641,703$, $p < 0.001$, partial $\eta^2 = 0.844$), and unsurprisingly, HC performed significantly better than SZ ($F(1,119) = 13.651$, $p < 0.001$, partial $\eta^2 = 0.103$) did. The interaction between set size and group was not significant ($F(1,119) = 0.229$, $p = 0.633$, partial $\eta^2 = 0.002$), indicating that set size equally affected the performance in both groups. Taken together, we replicated the widely documented VWM deficits in SZ.

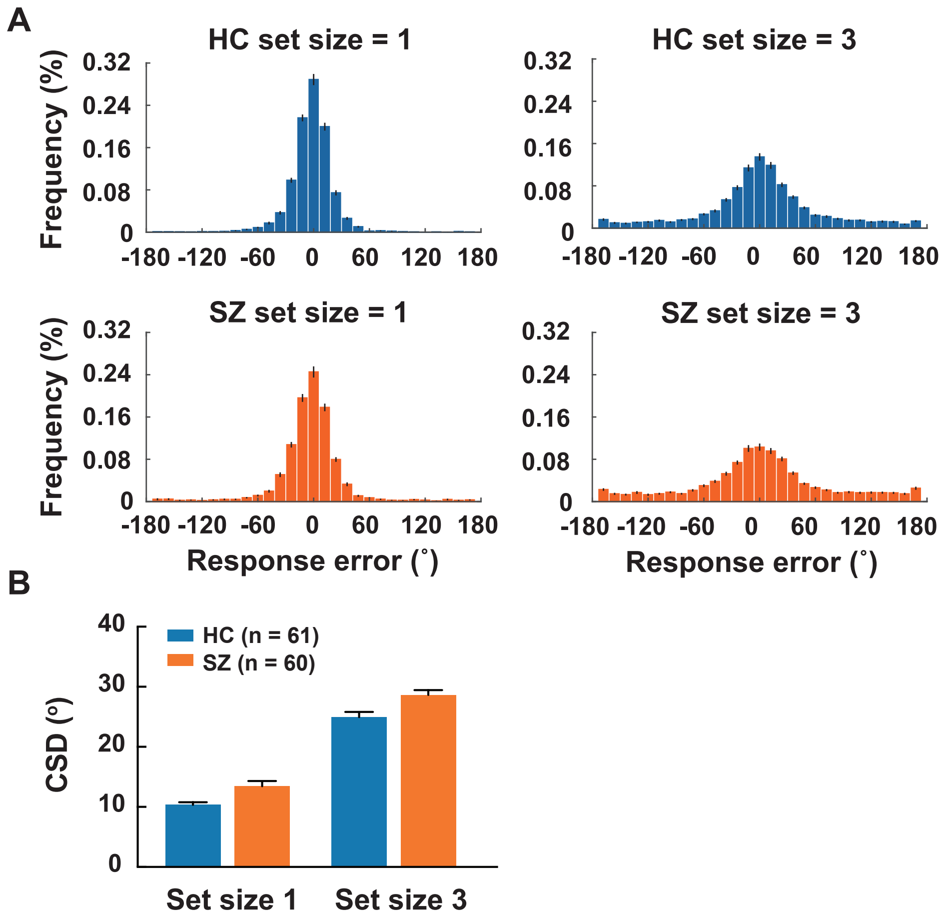

Figure 2. Visual working memory performance in SZ and HC. ***A.*** Histograms of circular response errors under set size 1 and 3 for both groups. ***B***. Circular standard deviations of response errors corresponding to Panel A. SZ show higher CSDs (i.e., worse performance) than HC. All error bars represent SEM across subjects.

Variable-precision model accounts for VWM behavior in both HC and SZ

To systematically compare the VWM performance of SZ and HZ, we evaluated almost all mainstream computational models of VWM. We provide some brief introductions here, and readers may consider to skip the following paragraph to directly reach the after results or go to Supplementary Notes 1&2 for detailed mathematical and intuitive explanations of the models, depending on the reading preference.

The first one is the item-limit (IL) model. The IL model assumes no uncertainty in the sensory encoding stage, and that each subject has a fixed memory capacity and a fixed response variability across set size levels [41]. The second one is the mixture (MIX) model, similar to the IL model but assuming response variability is set-size dependent [25,26]. Compared with the MIX model, the slots-plus-averaging (SA) model [37] further elaborates the idea that memory resources manifest as discrete chunks, and these chunks can be flexibly assigned to multiple items. We also explored a modified version of the SA model, dubbed cosSA model, which inherits the idea of discrete memory resources and further assumes that response bias is stimulus-dependent and can be described as empirically derived periodic functions. The fifth one is the equal-precision (EP) model, which is similar to the variable-precision (VP) model below but assumes that the memory resources are evenly distributed across items and trials [42,43]. The VP model proposes that memory resources are continuous, and the amount of resource assigned to individual items varies across items and trials. Note that the VP model does not include the capacity component thus we also constructed a variable-precision-with-capacity (VPcap) model that not only acknowledges the variable precision mechanisms and but also explicitly estimates the capacity of individual subjects. Note that the IL, MIX, SA and cosSA, and VPcap models have the parameter of capacity, and the EP and VP models do not. Here, capacity is operationally defined as the maximum number of items that can be stored in memory. Some items are out of memory if set size exceeds capacity, and the subject has to randomly guess the color if one of these items is probed.

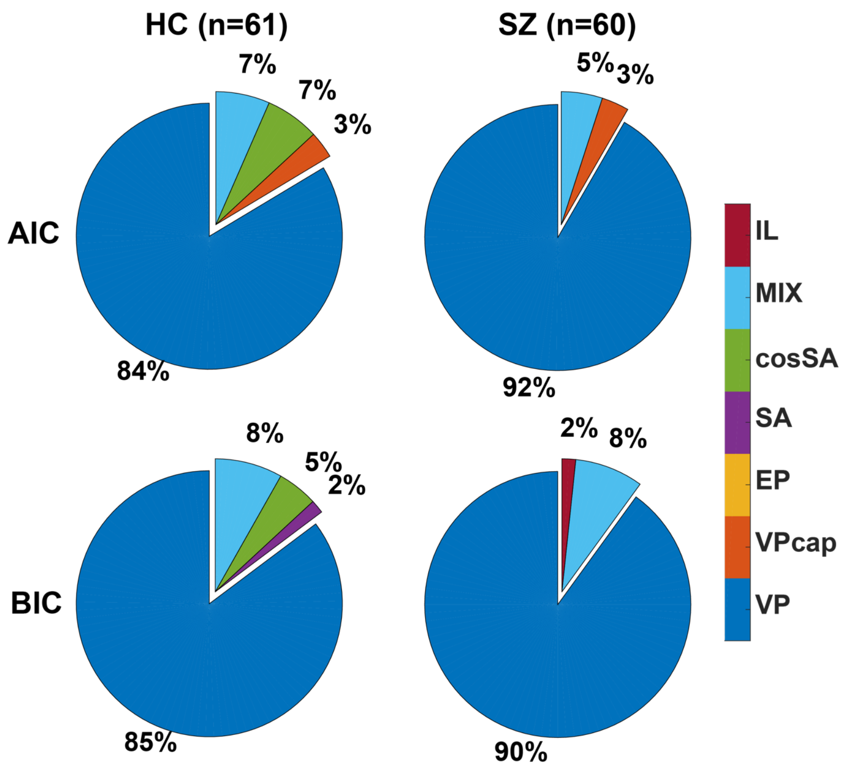

Figure 3. Model comparison results. We compared seven models in each subject. The pie charts illustrate the proportion of subjects for whom each model is their best-fitting model. The VP model is the best-fitting model for over 84% of subjects in both groups and under both AIC and BIC metrics. This result indicates both groups share a qualitatively similar internal process of VWM.

We compared all seven models using the Akaike information criterion (AIC) and the Bayesian information criterion (BIC) [44,45]. We found that (Fig. 3), among all models, the VP model was the best-fitting model for over 84% of subjects in the HC group under both metrics, replicating previous results in normal subjects [46,47]. Most importantly, the VP model (Fig. 4) was also the best-fitting model for over 90% of subjects in the SZ group. This result indicates that both groups use the same observer model to perform the task.

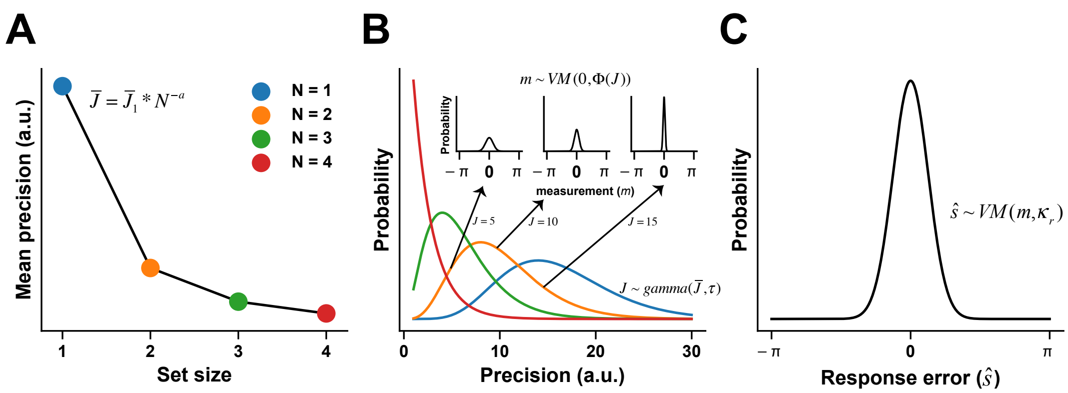

Figure 4. Variable-precision model of VWM. ***A***. Resource decay function. The VP model assumes that the mean resource ($\bar{J}$) for processing a single item declines as a power function of set size N, a trend characterized by two free parameters—initial resources ($\bar{J}_1$) and decaying exponent (a). ***B***. The resources across items or trials follow a gamma distribution with the mean resource ($\bar{J}_1$) determined by the resource decay function (panel A) and the resource allocation variability (τ). Larger amounts of resources (J) indicate higher precision and therefore generate narrower von Mises distributions (three small axes indicating the precision equals to 5, 10 and 15 respectively) of stimulus measurement (m). The widths of the von Mises distributions indicate the degree of trial-by-trial sensory uncertainty. ***C***. The eventual behavioral choice given the internal stimulus measurement (m) is also uncertain, following a von Mises distribution with the choice variability (κ_r) [80]. In the VP model, initial resources ($\bar{J}$), decaying exponent (a), resource allocation variability (τ) and choice variability (κ_r) are four free parameters to estimate (see details in SI and van den Berg *et al.* [46]). All numbers here are only for illustration purposes and not quantitatively related to the model fitting results in this paper.

It is worth highlighting two findings here. First, the superior performance of the VP model suggests the important role of variable precision in VWM processing. Second, we found that the VP model was better than the VPcap model. This result suggests that adding the capacity parameter in the VPcap model seems unnecessary from the modeling perspective. This result is also in line with the literature showing that a fixed capacity might not exist in VWM [48,49]. Although systematically examining the existence of a fixed capacity is beyond the scope of this paper, this result at least invites a rethink of whether memory capacity should be considered as a key factor that limits VWM performance in SZ.

Larger resource allocation variability in SZ

Analyses above have established that HC and SZ employ the qualitatively same observer model to complete the VWM task. Their behavioral differences thus should arise from the differences on some parameters in the observer model. We next compared the fitted parameters of the VP model in the two groups. Results showed that the two groups had comparable resource decay functions (Fig. 5A, initial resources, $t(119) = 0.689$, $p = 0.492$, $d = 0.125$; decaying exponent, $t(119) = 1.065$, $p = 0.289$, $d = 0.194$), indicating a similar trend of diminished memory resources as set size increases. SZ, however, had larger variability in allocating resources (Fig. 5B, resource allocation variability, $t(119) = 4.03$, $p = 9.87 \times 10^{-5}$, $d = 0.733$). This suggests that, although the two groups have on average the same amount of memory resources across different set size levels, SZ allocate the resources across items or trials in a more heterogeneous manner, with some items in some trials receiving considerably larger amounts and vice versa in other cases. This is theoretically suboptimal with respect to completing the task since the probe was randomly chosen among all presented items with an equal probability. The optimal strategy therefore should be to assign an equal amount of resources to every item and in every trial to tackle the unpredictable target. Furthermore, our VP model explicitly distinguishes the variability in processing items and the variability in exerting a behavioral choice (e.g., motor or decision noise). We found no significant group difference in the choice variability (Fig. 5C, $t(119) = 1.7034$, $p = 0.091$, $d = 0.31$), excluding the possibility that the atypical performance of SZ arises from larger variability at the choice stage.

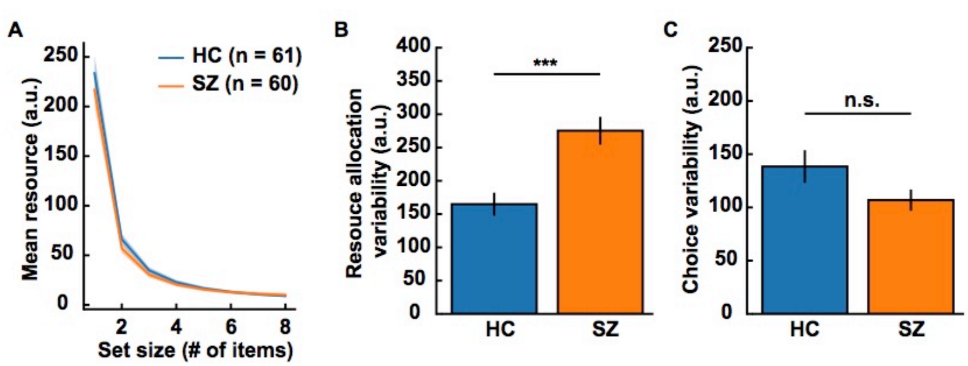

Figure 5. Fitted parameters of the VP model. No significant group differences are noted between two groups in resource decay functions (panel A), and choice variability (panel C). SZ have larger resource allocation variability than

HC (panel B). The individual resource decay functions are computed by $\bar{J} = \bar{J}_1 * N^{-a}$, where N is the set size, $\bar{J}_1$ and a are the estimated initial resources and the decaying exponent of one subject. The solid lines represent the averaged resource decay functions across subjects. The shaded areas in panel A and all error bars in panel B and C represent ±SEM across subjects. Significance symbol conventions are ***: $p < 0.001$; n.s.: non-significant.

No capacity difference between HC and SZ

Although the VP model is the most appropriate model for both groups, we believe it is also valuable to examine other suboptimal models for several reasons. First, the VP model does not have the concept of capacity. Thus, we cannot completely rule out the influence of capacity. One might argue that resource allocation variability and limited capacity might jointly manifest in SZ and a hybrid model that aggregates the two factors might yield a better explanation. Second, conclusions based on a single model might be unreliable as its fitted parameters may arise from specific model settings or possible idiosyncratic model fitting processes.

First, we emphasize that the VPcap model is such a hybrid model that accommodates both the variable precision mechanism and a fixed capacity. The results from the VPcap model largely replicated the results of the VP model. Again, we found a significantly larger resource allocation variability in SZ ($t(119) = 3.891$, $p = 1.65 \times 10^{-4}$, $d = 0.707$), see full statistical results in Supplementary Note 4). This result suggests that the effect of resource allocation variability is quite robust even though we alter the model structure.

We further examined the estimated capacity of all subjects in all models that contain the capacity parameter (i.e., IL, MIX, SA, cosSA, and VPcap models). Consistently, none of the models showed decreased capacity in SZ (see full stats in Supplementary Note 4 and Supplementary Figure 4). This result further rules out capacity deficits in SZ.

In sum, we found robustly larger resource allocation variability in SZ in both the VP and the VPcap models. Also, we found no evidence for decreased capacity in SZ in all models that include the capacity parameter. These results directly challenge the widely accepted decreased-capacity account and highlight the role of resource allocation variability in VWM deficits of SZ.

Resource allocation variability predicts the severity of schizophrenic symptoms

We next turned to investigate whether the results from the VP model can predict clinical symptoms. A set of correlational analyses was carried out to link the estimated resource allocation variability to the schizophrenia symptomatology in each subject (BPRS, SANS, and SAPS).

We noticed that the estimated resource allocation variability of individual subjects correlates with their BPRS scores (Fig. 6A, r = 0.259, p = 0.045) and the SANS scores (Fig. 6B, r = 0.302, p = 0.019) in SZ. No significant correlation was noted on the SAPS scores (Fig. 6C, r = -0.121, p = 0.358). These results suggest that resource allocation variability not only is the key factor describing VWM behavior in SZ but also can quantitatively predict the severity of clinically measured symptoms.

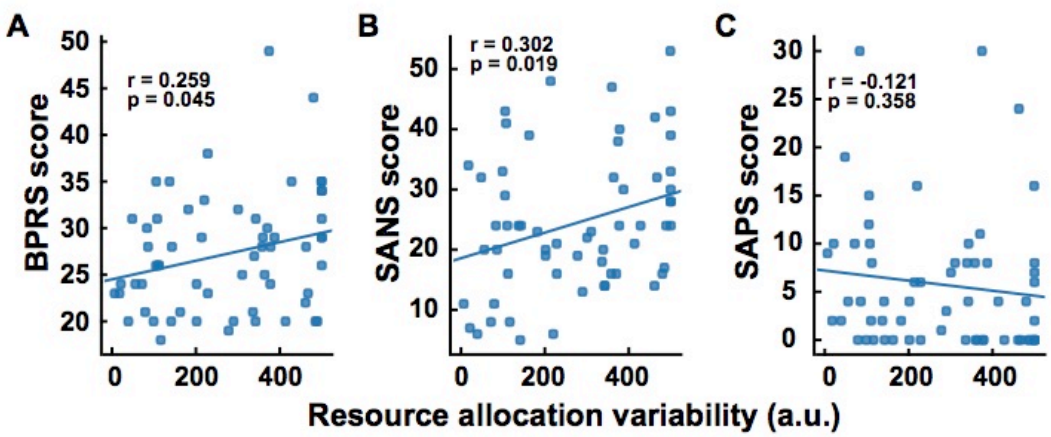

Figure 6. Individual differences in resource allocation variability predict the scores in symptom assessments. Estimated resource allocation variability values in the SZ group significantly correlates with their scores on BPRS (panel A) and SANS (negative symptoms, panel B) but not on SAPS (positive symptoms, panel C).

Discussion

The mechanisms of VWM deficits in schizophrenia have been a matter of debate over the past few years. One widely accepted view proposes decreased capacity as the major cause of the deficits in SZ. In the present study, we re-examine this conclusion by comparing the performance of SZ and HC using all mainstream computational models of VWM proposed so far. We first establish that the VP model is the best model to characterize performance of both groups, indicating a qualitative similar internal process in both groups. We then further evaluate different components in the VP model as well as other suboptimal models, with special focuses on memory capacity and the declining trend of mean precision as a function of set size. Surprisingly, we find that SZ and HC differ in none of these two diagnostic features of VWM. Interestingly, we find that SZ have larger variability in allocating memory resources. Furthermore, individual differences in resource allocation variability predict variation of patients' symptom severity, highlighting the clinical functionality of this factor. Taken together, our results challenge the long-standing decreased-capacity explanation for the VWM deficits in schizophrenia and propose for the first time that resource allocation variability is the key factor that limits their performance.

A large body of literature has documented that SZ perform poorly in various forms of working memory tasks [2,3,50,51]. They reached the same conclusion: memory capacity is decreased in schizophrenia. However, through a careful examination of the literature, we find that the definition of capacity varies substantially across studies. Many studies directly equated worse performance with decreased capacity without quantitatively demonstrating how capacity modulates performance. For example, memory capacity was defined as the number of digits that can be recalled in the longest strand in digit span tasks [12]. In N-back tasks, capacity was defined as the number of backs corresponding to a certain accuracy level [14–16]. Moreover, the calculation of capacity resembled the d-prime metric in change detection tasks [22–24,41,52]. The majority of these metrics are behavioral thresholds related to capacity rather than direct quantifications of capacity. Although these metrics indeed suggest worse performance in SZ, they cannot directly reveal decreased capacity given the presence of other components such as memory resource or choice variability. It is still unclear how these components jointly determine performance. This is partly because we lack appropriate computational models for the majority of the tasks. The VP model is advantageous as it describes the generative process of the delay-estimation task and the change-detection task [46]. As such, it allows to disassociate the effect of capacity from other VWM components.

The most notable result in our study is that no group difference is discovered in capacity in all models that estimate capacity. One potential limitation here might be that we only tested set size 1 and 3 given the limited number of trials we were able to collect on SZ patients. We acknowledge that high set size levels that challenge the subjects' VWM ability would lead to more accurate estimates of capacity. But we tended to be conservative when designing the experiment as SZ had already shown significant guessing behavior on set size 3 in our pilot experiment (also see Fig. 2A). Moreover, the fact that no capacity differences in all models are unlikely driven by the parameter setting in a particular model. One might also argue that adding the capacity parameter in for example the SA and MIX models might not significantly improve goodness of fit but will be penalized by AIC and BIC metrics, rendering worse models in terms of model comparison. We exclude this possibility by performing model comparisons using AIC and BIC without considering the capacity parameter (see Supplementary Note 3). Results replicated our main conclusions here. Future studies might need to test more conditions and more behavioral tasks.

Only a few studies have quantitatively estimated capacity and precision in schizophrenia. Gold et al [25] employed the same delay-estimation task as in our study and estimated individual's capacity and precision using the MIX model. Results in that study echoed the decreased-capacity theory. The MIX model assumes that response errors arise from a mixture distribution that combines a von Mises distribution whose variance reflects memory precision, and a uniform distribution that accounts for the random guessing if set size exceeds capacity. The MIX model, however, does not consider two important factors. First, the model assumes an equal precision across items in memory. Second, the model does not separate the variability for processing stimuli (i.e., sensory uncertainty, κ in

Supplementary Eq. S5) and the variability in exertion of a choice (i.e., choice uncertainty, κ_r in Supplementary Eq. S6). Such distinction is important since it highlights different types of uncertainty in encoding and decoding stages of VWM. Mathematically, these two types of uncertainty can be distinguished by manipulating set size since the encoding variability depends on set size but the choice variability does not. The issues of the MIX model have been symmetrically addressed in recent work [53].

Compared with capacity and precision—the two diagnostic features of VWM, resource allocation variability emerges as a new concept in VWM. It describes the heterogeneity of allocating resources across multiple items and trials. Recent work suggests that such variability might not only manifest in VWM and but also act as a ubiquitous mechanism when processing multiple objects in vision [54]. We speculate that resource allocation variability reflects the stability of attentional control when the brain processes multiple objects. Two aspects of available evidence support this argument. First, it has been shown that attention and WM are two core components of executive control and tightly linked with each other [55,56]. Second, schizophrenia is known to have deficits in top-down attentional modulation [51,55]. Particularly, recent studies discovered the phenomenon of spatial hyperfocusing in schizophrenia patients [19,57–59]. If schizophrenia patients overly attend to one item and ignore others in the memory encoding stage, unbalanced resource allocation will likely occur. But we want to emphasize that such variability is not equivalent to attentional lapse. A higher attentional lapse rate will lead to overall fewer resources, a phenomenon we did not observe in our study.

What are the neural mechanisms of this resource allocation variability? Recent neurophysiological studies proposed that the neural representation of a stimulus may follow a doubly stochastic process [60,61], which suggests that the variability in encoding precision is a consequence of trial-to-trial and item-to-item fluctuations in attentional gain [32,46,62]. A recent study combined functional magnetic resonance imaging and the VP model, showing that the superior intraparietal sulcus (IPS) is the cortical locus that controls the resource allocation [63]. Interestingly, schizophrenia patients have been known to have IPS deficits [64]. Note that besides top-down factors, we cannot rule out the contribution of bottom-up neural noise in perceptual and cognitive processing [60,61], as found in several other mental diseases [33–36].

The current results also reveal links between resource allocation variability and patients' negative symptoms, but not positive symptoms (Fig. 6). These findings are consistent with several experimental and meta-analysis studies claiming dissociable mechanisms underlying the cluster of negative symptoms versus that of positive symptoms [65–68]. More broadly, a growing collection of evidence suggests that visual perceptual deficits in schizophrenic patients are more likely to link to negative rather than positive symptom severity [69–73]. Negative symptoms in turn might produce improvised social functioning. Humans depend heavily on VWM to interact with multiple agents and complete social tasks. Deficits in distributing processing resources over multiple agents therefore might cause disadvantages in social cognition.

In conclusion, our study proposes a new explanation that the resource allocation variability accounts for the atypical VWM performance in schizophrenia. This view differs from the decreased-capacity theory and provides a new direction for future studies that attempt to promote diagnosis and rehabilitation for schizophrenic patients.

Methods

Ethics Statement.

All experimental protocols were approved by the institutional review board at the East China Normal University. All research was performed in accordance with relevant guidelines and regulations. Informed written consent was obtained from all participants.

Subjects.

61 HC and 60 SZ participated in the study. SZ were clinically stable inpatients (N = 33) and outpatients (N = 27) who met DSM-IV criteria [74] for schizophrenia. All patients were receiving antipsychotic medication (2 first-generation, 43 second-

generation, 15 both). Symptom severity was evaluated by the Brief Psychiatric Rating Scale (BPRS) [75], the Scale for the Assessment of Negative (SANS) and Positive Symptoms (SAPS) [76,77]. HC were recruited by advertisement. All HC had no current diagnosis of axis 1 or 2 disorders as well as no family history of psychosis nor substance abuse or dependence. All subjects are right-handed with normal sight and color perception.

The two groups were matched in age ($t(119) = 1.58$, $p = 0.118$, $d = 0.284$), gender (31 females and 29 males) and education level of parents ($t(119) = 0.257$, $p = 0.798$, $d = 0.047$). Inevitably, the SZ had fewer years of education than the HC ($t(119) = 5.51$, $p = 2.09 \times 10^{-7}$, $d = 1.00$). The detailed demographic information is summarized in the Table 1.

Table 1. Demographics and clinical information of people with schizophrenia (SZ) and healthy control subjects (HC)

	SZ (N = 60)		HC (N = 61)	
	Mean	SD	Mean	SD
age	35.67	6.58	33.82	9.90
range	23-48	n/a	21-57	n/a
Female/male	31/29	n/a	29/32	n/a
Inpatient/outpatient	33/27	n/a	n/a	n/a
Subject’s education (in years)	12.03	2.24	15.13	3.70
Paternal education (in years) [a]	9.89	2.53	9.76	2.95
Maternal education (in years)	9.62	2.91	9.29	3.63
BPRS	27.25	6.27	n/a	n/a
SAPS	5.77	7.02	n/a	n/a
SANS	24.43	11.45	n/a	n/a

[a] Average of mother’s and father’s years of education

BPRS: Brief Psychiatric Rating Scale [75]; SAPS: Scale for the Assessment of Positive Symptoms [77]; SANS: Scale for the Assessment of Negative Symptoms [76].

Stimuli and Task.

The subjects sat 50 cm away from an LCD monitor. All stimuli were generated by Matlab 8.1 and Psychtoolbox 3 [78,79], and then presented on a LCD monitor.

Color delay-estimation VWM task

In the color delay-estimation VWM task (Fig. 1), each trial began with a fixation cross presented at center-of-gaze for a duration randomly chosen from a sequence of 300, 350, 400, 450 and 500 ms. Subjects shall keep their fixation on the cross throughout the whole experiment. A set of colored squares (set size = 1 or 3) was shown on an invisible circle with 4° radius. Our pilot experiment showed that SZ patients exhibit a high dropout rate if the task is longer than 30 mins or too hard (i.e., set size > 4). We therefore limited our task to set size level 1 and 3. The sample array lasted 500 ms. Each square was 1.5° × 1.5° of visual angle. Their colors were randomly selected from the 180 colors that are equally distributed along the wheel representing the CIE L*a*b color space. The color wheel was centered at (L = 70, a = 20, b = 38) with a radius of 60 in the color space [37]. The sample array then disappeared and was followed by a 900 ms blank period for memory retention. After the delay, an equal number of outlined squares were shown at the same location of each sample array item, with one of them bolded as the probe. In the meantime, a randomly rotated color wheel was shown. The color wheel was 2.1° thick and centered on the monitor with the inner and the outer radius as 7.8° and 9.8° respectively. Subjects were asked to choose the remembered color of the probe by clicking a color on the color wheel using a computer mouse. Subjects shall choose the color as precisely as possible and response time was not constrained. Every subject completed 2 blocks for the set size 1 and 3, respectively. The order of the two blocks was counterbalanced across subjects. Each block had 80 trials. The difference between the reported color and the true color of the target is considered as the response error.

Data availability statement

The data that support the findings of this study are available from the corresponding author upon reasonable request.

Acknowledgments

We thank Zheng Ma, Ting Qian and Haojiang Ying for their invaluable comments on the manuscript. This work was supported by the National Social Science Foundation of China (17ZDA323), the National Key Fundamental Research Program of China (2013CB329501), the Major Program of Science and Technology Commission Shanghai Municipal (17JC1404100), the Fundamental Research Funds for the Central Universities (2018ECNU-QKT015), and the NYU-ECNU Institute of Brain and Cognitive Science at NYU (YK).

Author contributions

Y. K., Y. Z. and X. R. designed the experiments. X. R. and L. Z. performed the experiments. Y. Z., T.M. and R-Y. Z. analyzed the data, R-Y. Z. and wrote the manuscript in consultation with Y. K. and L. Z.

References

1. Gold, J. M., Randolph, C. & Carpenter, C. Auditory working memory and Wisconsin Card Sorting Test Performance in Schizophrenia. *Arch. Gen. Psychiatry* **54,** 159–165 (1997).

2. Lee, J. & Park, S. Working Memory Impairments in Schizophrenia: A Meta-Analysis. *J. Abnorm. Psychol.* **114,** 599–611 (2005).

3. Forbes, N. F., Carrick, L. A., McIntosh, A. M. & Lawrie, S. M. Working memory in schizophrenia: a meta-analysis. *Psychol. Med.* **39,** 889–905 (2009).

4. Goldman-Rakic, P. S. Working memory dysfunction in schizophrenia. *J. Neuropsychiatry Clin. Neurosci.* **6,** 348–357 (1994).

5. Mayer, R. E. & Moreno, R. A split-attention effect in multimedia learning: Evidence for dual processing systems in working memory. *J. Educ. Psychol.* **90,** 312–320 (1998).

6. Postle, B. R. Working memory as an emergent property of the mind and brain. *Neuroscience* **139,** 23–38 (2006).

7. Nee, D. E. *et al.* A meta-Analysis of executive components of working memory. *Cereb. Cortex* **23,** 264–282 (2013).

8. Luck, S. J. & Vogel, E. K. Visual working memory capacity: From psychophysics and neurobiology to individual differences. *Trends Cogn. Sci.* **17,** 391–400 (2013).

9. Coleman, M. J., Krastoshevsky, O., Tu, X., Mendell, N. R. & Levy, D. L. The effects of perceptual encoding on the magnitude of object working memory impairment in schizophrenia. *Schizophr. Res.* **139,** 60–65 (2012).

10. Leonard, C. J. *et al.* Testing sensory and cognitive explanations of the antisaccade deficit in schizophrenia. *J. Abnorm. Psychol.* **122,** 1111–1120 (2013).

11. Johnson, M. K. *et al.* The relationship between working memory capacity and broad measures of cognitive ability in healthy adults and people with schizophrenia. *Neuropsychology* **27,** 220–229 (2013).

12. Conklin, H. M. Verbal Working Memory Impairment in Schizophrenia Patients and Their First-Degree Relatives: Evidence From the Digit Span Task. *Am. J. Psychiatry* **157,** 275–277 (2000).
13. Chey, J., Lee, J., Kim, Y.-S., Kwon, S.-M. & Shin, Y.-M. Spatial working memory span, delayed response and executive function in schizophrenia. *Psychiatry Res.* **110,** 259–271 (2002).
14. Callicott, J. Functional Magnetic Resonance Imaging Brain Mapping in Psychiatry: Methodological Issues Illustrated in a Study of Working Memory in Schizophrenia. *Neuropsychopharmacology* **18,** 186–196 (1998).
15. Barch, D. M., Csernansky, J. G., Conturo, T. & Snyder, A. Z. Working and long-term memory deficits in schizophrenia: Is there a common prefrontal mechanism? *J. Abnorm. Psychol.* **111,** 478–494 (2002).
16. Jansma, J. M., Ramsey, N. F., Van Der Wee, N. J. A. & Kahn, R. S. Working memory capacity in schizophrenia: A parametric fMRI study. *Schizophr. Res.* **68,** 159–171 (2004).
17. Park, S. Schizophrenics Show Spatial Working Memory Deficits. *Arch. Gen. Psychiatry* **49,** 975 (1992).
18. Keedy, S. K., Ebens, C. L., Keshavan, M. S. & Sweeney, J. A. Functional magnetic resonance imaging studies of eye movements in first episode schizophrenia: Smooth pursuit, visually guided saccades and the oculomotor delayed response task. *Psychiatry Res.* **146,** 199–211 (2006).
19. Sawaki, R. *et al.* Hyperfocusing of attention on goal-related information in schizophrenia: Evidence from electrophysiology. *J. Abnorm. Psychol.* **126,** 106–116 (2017).
20. Gold, J. M., Wilk, C. M., McMahon, R. P., Buchanan, R. W. & Luck, S. J. Working memory for visual features and conjunctions in schizophrenia. *J. Abnorm. Psychol.* **112,** 61–71 (2003).
21. Lencz, T. *et al.* Impairments in perceptual competency and maintenance on a visual delayed match-to-sample test in first-episode schizophrenia. *Arch. Gen. Psychiatry* **60,** 238–243 (2003).

22. Erickson, M. A. *et al.* Impaired Working Memory Capacity Is Not Caused by Failures of Selective Attention in Schizophrenia. *Schizophr. Bull.* **41,** 366–373 (2015).

23. Erickson, M. A. *et al.* Enhanced vulnerability to distraction does not account for working memory capacity reduction in people with schizophrenia. *Schizophr. Res. Cogn.* **1,** 149–154 (2014).

24. Leonard, C. J. *et al.* Toward the Neural Mechanisms of Reduced Working Memory Capacity in Schizophrenia. *Cereb. Cortex* **23,** 1582–1592 (2013).

25. Gold, J. M. *et al.* Reduced Capacity but Spared Precision and Maintenance of Working Memory Representations in Schizophrenia. *Arch. Gen. Psychiatry* **67,** 570–577 (2010).

26. Xie, W. *et al.* Schizotypy is associated with reduced mnemonic precision in visual working memory. *Schizophr. Res.* **193,** 91–97 (2018).

27. Starc, M. *et al.* Schizophrenia is associated with a pattern of spatial working memory deficits consistent with cortical disinhibition. *Schizophr. Res.* **181,** 107–116 (2017).

28. Ma, W. J., Husain, M. & Bays, P. M. Changing concepts of working memory. *Nat. Neurosci.* **17,** 347–356 (2014).

29. Bialek, W. Physical Limits to Sensation and Perception. *Annu. Rev. Biophys. Biophys. Chem.* **16,** 455–478 (1987).

30. Rolls, E. T. & Deco, G. *The Noisy Brain: Stochastic Dynamics as a Principle of Brain Function*. (Oxford University Press, 2010).

31. Faisal, A. A., Selen, L. P. J. & Wolpert, D. M. Noise in the nervous system. *Nature Reviews Neuroscience* **9,** 292–303 (2008).

32. Goris, R. L. T., Movshon, J. A. & Simoncelli, E. P. Partitioning neuronal variability. *Nat. Neurosci.* **17,** 858–865 (2014).

33. Dinstein, I. *et al.* Unreliable Evoked Responses in Autism. *Neuron* **75,** 981–991 (2012).

34. Park, W. J., Schauder, K. B., Zhang, R., Bennetto, L. & Tadin, D. High internal noise and poor external noise filtering characterize perception in autism spectrum disorder. *Sci. Rep.* **7,** 17584 (2017).

35. Sperling, A. J., Lu, Z.-L., Manis, F. R. & Seidenberg, M. S. Deficits in perceptual noise exclusion in developmental dyslexia. *Nat. Neurosci.* **8,** 862–863 (2005).
36. Bubl, E. *et al.* Elevated Background Noise in Adult Attention Deficit Hyperactivity Disorder Is Associated with Inattention. *PLoS One* **10,** e0118271 (2015).
37. Zhang, W. & Luck, S. J. Discrete fixed-resolution representations in visual working memory. *Nature* **453,** 233–235 (2008).
38. Zhang, W. & Luck, S. J. Sudden Death and Gradual Decay in Visual Working Memory: Research Report. *Psychol. Sci.* **20,** 423–428 (2009).
39. Zhang, W. & Luck, S. J. The number and quality of representations in working memory. *Psychol. Sci.* **22,** 1434–1441 (2011).
40. Foster, J. J., Bsales, E. M., Jaffe, R. J. & Awh, E. Alpha-Band Activity Reveals Spontaneous Representations of Spatial Position in Visual Working Memory. *Curr. Biol.* **27,** 3216–3223.e6 (2017).
41. Pashler, H. Familiarity and visual change detection. *Percept. Psychophys.* **44,** 369–378 (1988).
42. Palmer, J. Attentional limits on the perception and memory of visual information. *J. Exp. Psychol. Hum. Percept. Perform.* **16,** 332–350 (1990).
43. Shaw, M. in *Attention and Performance* (ed. Nickerson, R.) 227–296 (Erlbaum, 1980).
44. Wit, E., van den Heuvel, E. & Romeijn, J. W. 'All models are wrong. ': An introduction to model uncertainty. *Stat. Neerl.* **66,** 217–236 (2012).
45. Burnham, K. P. & Anderson, D. R. *Model Selection and Multimodel Inference: A Practical Information-Theoretic Approach*. *Ecological Modelling* **172,** (Springer-Verlag, 2002).
46. van den Berg, R., Shin, H., Chou, W.-C., George, R. & Ma, W. J. Variability in encoding precision accounts for visual short-term memory limitations. *Proc. Natl. Acad. Sci.* **109,** 8780–8785 (2012).
47. van den Berg, R., Awh, E. & Ma, W. J. Factorial comparison of working memory models. *Psychol. Rev.* **121,** 124–149 (2014).

48. Bays, P. M. & Husain, M. Dynamic Shifts of Limited Working Memory Resources in Human Vision. *Science (80-.).* **321,** 851–854 (2008).

49. Bays, P. M., Catalao, R. F. G. & Husain, M. The precision of visual working memory is set by allocation of a shared resource. *J. Vis.* **9,** 7.1-11 (2009).

50. Shakow, D. The Worcester State Hospital research on schizophrenia (1927-1946). *J. Abnorm. Psychol.* **80,** 67–110 (1972).

51. Gold, J. M., Hahn, B., Strauss, G. P. & Waltz, J. A. Turning it upside down: Areas of preserved cognitive function in schizophrenia. *Neuropsychol. Rev.* **19,** 294–311 (2009).

52. Cowan, N. The magical number 4 in short-term memory: A reconsideration of mental storage capacity. *Behav. Brain Sci.* **24,** 87–114 (2001).

53. Ma, W. J. Problematic usage of the Zhang and Luck mixture model. *bioRxiv* (2018). doi:10.1101/268961

54. Shen, S. & Ma, W. J. Variable precision in visual perception. *bioRxiv* 153650 (2018). doi:10.1101/153650

55. Gold, J. M. *et al.* Selective Attention, Working Memory, and Executive Function as Potential Independent Sources of Cognitive Dysfunction in Schizophrenia. *Schizophr. Bull.* **44,** 1227–1234 (2018).

56. Christophel, T. B., Iamshchinina, P., Yan, C., Allefeld, C. & Haynes, J. D. Cortical specialization for attended versus unattended working memory. *Nat. Neurosci.* **21,** 494–496 (2018).

57. Fuller, R. L. *et al.* Impaired control of visual attention in schizophrenia. *J. Abnorm. Psychol.* **115,** 266–275 (2006).

58. Kreither, J. *et al.* Electrophysiological Evidence for Hyperfocusing of Spatial Attention in Schizophrenia. *J. Neurosci.* **37,** 3813–3823 (2017).

59. Luck, S. J. *et al.* Hyperfocusing in schizophrenia: Evidence from interactions between working memory and eye movements. *J. Abnorm. Psychol.* **123,** 783–795 (2014).

60. Churchland, A. K. *et al.* Variance as a Signature of Neural Computations during Decision Making. *Neuron* **69,** 818–831 (2011).

61. Churchland, M. M. *et al.* Stimulus onset quenches neural variability: a widespread cortical phenomenon. *Nat. Neurosci.* **13,** 369–378 (2010).

62. Nienborg, H. & Cumming, B. G. Decision-related activity in sensory neurons reflects more than a neuron's causal effect. *Nature* **459,** 89–92 (2009).

63. Galeano Weber, E. M., Peters, B., Hahn, T., Bledowski, C. & Fiebach, C. J. Superior Intraparietal Sulcus Controls the Variability of Visual Working Memory Precision. *J. Neurosci.* **36,** 5623–5635 (2016).

64. Zhou, S.-Y. *et al.* Parietal lobe volume deficits in schizophrenia spectrum disorders. *Schizophr. Res.* **89,** 35–48 (2007).

65. de Gracia Dominguez, M., Viechtbauer, W., Simons, C. J. P., van Os, J. & Krabbendam, L. Are Psychotic Psychopathology and Neurocognition Orthogonal? A Systematic Review of Their Associations. *Psychol. Bull.* **135,** 157–171 (2009).

66. Cameron, A. M. *et al.* Working memory correlates of three symptom clusters in schizophrenia. *Psychiatry Res.* **110,** 49–61 (2002).

67. Carter, C. *et al.* Spatial working memory deficits and their relationship to negative symptoms in unmedicated schizophrenia patients. *Biol. Psychiatry* **40,** 930–932 (1996).

68. Park, S., Püschel, J., Sauter, B. H., Rentsch, M. & Hell, D. Visual object working memory function and clinical symptoms in schizophrenia. *Schizophr. Res.* **59,** 261–268 (2003).

69. Cadenhead, K. S. *et al.* Information processing deficits of schizophrenia patients: Relationship to clinical ratings, gender and medication status. *Schizophr. Res.* **28,** 51–62 (1997).

70. Butler, P. D. & Javitt, D. C. Early-stage visual processing deficits in schizophrenia. *Current Opinion in Psychiatry* **18,** 151–157 (2005).

71. Kéri, S., Kiss, I., Kelemen, O., Benedek, G. & Janka, Z. Anomalous visual experiences, negative symptoms, perceptual organization and the magnocellular pathway in schizophrenia: A shared construct? *Psychol. Med.* **35,** 1445–1455 (2005).

72. Slaghuis, W. L. Spatio-temporal luminance contrast sensitivity and visual backward masking in schizophrenia. *Exp. brain Res.* **156,** 196–211 (2004).

73. Slaghuis, W. L. & Bishop, A. M. Luminance flicker sensitivity in positive- and negative-symptom schizophrenia. *Exp. Brain Res.* **138,** 88–99 (2001).

74. American Psychiatric Association. *Diagnostic and statistical manual of mental disorders (4th ed.)*. *American Psychiatric Publishing* (1994).

75. Overall, J. E. & Gorham, D. R. The Brief Psychiatric Rating Scale. *Psychol. Rep.* **10,** 799–812 (1962).

76. Andreasen, N. C. *The Scale for the Assessment of Negative Symptoms (SANS)*. *University of Iowa* (1983).

77. Andreasen, N. C. *The Scale for the Assessment of Positive Symptoms (SAPS)*. *University of Iowa* (1984).

78. Brainard, D. H. The Psychophysics Toolbox. *Spat. Vis.* **10,** 433–436 (1997).

79. Pelli, D. G. The VideoToolbox software for visual psychophysics: Transforming numbers into movies. *Spat. Vis.* **10,** 437–442 (1997).

80. Osborne, L. C., Lisberger, S. G. & Bialek, W. A sensory source for motor variation. *Nature* **437,** 412–416 (2005).

Supplementary materials for

Atypically larger variability of resource allocation accounts for visual working memory deficits in schizophrenia

Yi-Jie Zhao, Tianye Ma, Xuemei Ran, Li Zhang, Ru-Yuan Zhang*, Yixuan Ku*

Correspondence:

Yixuan Ku: yxku@psy.ecnu.edu.cn

Ru-Yuan Zhang zhan1217@umn.edu

This PDF file includes:

Supplementary Note 1: Computational models of VWM

Variable-precision model. The variable-precision (VP) model has been shown as the state-of-the-art computational model of VWM. Details of the VP model have been documented in several previous studies [1,2] and the model codes are publicly available (http://www.cns.nyu.edu/malab/resources.html).

The VP model assumes a resource decaying function describing the decreasing trend of mean memory resource ($\overline{J}$) assigned to individual items as the set size (N) increases [3,4]:

$$\overline{J} = \overline{J_1} * N^{-a} \ , \tag{S1}$$

where $\overline{J_1}$ is the initial resources when only 1 item ($N = 1$) should be memorized and a is the decaying exponent. The key component of the VP model is that the memory resources J across items and trials follow a Gamma distribution with the mean $\overline{J}$ and the scale parameter τ:

$$J \sim Gamma(\overline{J}, \tau) \ , \tag{S2}$$

Intuitively, a larger τ indicates a more uneven distribution of memory resources across items or trials, with some items in some trials receiving a larger amount of resources while others receive comparative fewer. Note that a larger amount of memory resource produces a higher precision. Thus, we do not explicitly distinguish resource and precision and denote them as J. Defining precision as Fisher information [5], precision J can be linked to the variance of the von Mises distribution of sensory measurement:

$$J = \kappa \frac{I_1(\kappa)}{I_0(\kappa)}, \tag{S3}$$

where I_0 and I_1 are modified Bessel functions of the first kind of order 0 and 1 respectively, with the concentration parameter κ. Eq. S3 specifies a one-on-one mapping between precision J and variance κ. We can rewrite their relationship as:

$$\kappa = \Phi(J) \ , \tag{S4}$$

where Φ is the mapping function. The distribution of sensory measurement (m) given the input stimulus (s) can be written as:

$$p(m \mid s) = \frac{1}{2\pi I_0(\kappa)} e^{\kappa \cos(m-s)} \equiv VM(m; s, \kappa), \tag{S5}$$

We further assume that the reported color ($\hat{s}$) by participants also follows a von Mises distribution:

$$p(\hat{s} \mid m) = \frac{1}{2\pi I_0(\kappa_r)} e^{\kappa_r \cos(\hat{s}-m)} \equiv VM(\hat{s}; m, \kappa_r), \tag{S6}$$

where k_r represents the variability at the choice stage.

Given the four free parameters and stimulus color s in a trial, we can derive the probability of the observed response in a trial by marginalizing over sensory measurement m and variable precision J:

$$\begin{aligned} p\left(\hat{s} \mid s;\, \bar{J}, \tau\right) &= \int p\left(\hat{s} \mid s; J\right) p\left(J \mid \bar{J}; \tau\right) dJ \\ &= \int VM\left(\hat{s}; s, \Phi\left(J\right)\right) Gamma\left(J; \bar{J}, \tau\right) dJ \\ &= \iint VM\left(\hat{s}; m, \kappa_r\right) VM\left(m; s, \Phi\left(J\right)\right) Gamma\left(J; \bar{J}, \tau\right) dJdm \\ &= \int \frac{I_0\left(\sqrt{\Phi\left(J\right)^2 + \kappa_r^2 + 2\Phi\left(J\right)\kappa_r cos\left(s-\hat{s}\right)}\right)}{2\pi I_0\left(\kappa_r\right) I_0\left(\Phi\left(J\right)\right)} Gamma\left(J; \bar{J}, \tau\right) dJ \end{aligned},$$

(S7)

Note that in Eq. S7, sensory measurement (m) can be analytically eliminated. Since precision J is a random variable across items and trials, we sampled it 10000 times from the Gamma distribution with mean $\bar{J}$ and scale parameter τ. Note that van den Berg *et al.* [1] confirmed that 500 samples are enough in the model fitting. We then used all the samples to calculate response probability in each trial.

Taken together, this VP model has four free parameters: $\bar{J}_1$, a, τ and κ_r.

Variable-precision-with-capacity model. The variable-precision-with-capacity (VPcap) model inherits all parameters and the structure of the VP model above, except that an additional capacity parameter (K) is introduced to estimate the memory capacity of individuals. If the set size N is smaller than capacity K, the VPcap model is identical to the VP model. If the set size N exceeds the capacity K, the model assumes that the probe is stored in the VWM with the probability K/N, and out of memory with the probability

1- *K*/*N*. In the latter case, a participant randomly guesses a color. The response probability therefore can be written as:

$$p(\hat{s} \mid s) = \begin{cases} \dfrac{K}{N} p(\hat{s} \mid s; \bar{J}, \tau) + (1 - \dfrac{K}{N}) \dfrac{1}{2\pi}, & K <= N \\ p(\hat{s} \mid s; \bar{J}, \tau), & K > N \end{cases}, \tag{S8}$$

where $p(\hat{s} \mid s; \bar{J}, \tau)$ is defined in Eq. S7. In essence, the VPcap model is a mixture model of the VP model and a random guessing process when the set size exceeds the participant's capacity. The VPcap model has five parameters, four as the same in the VP model and the additional capacity parameter (*K*).

Item-limit model. The item-limit (IL) model assumes no uncertainty in the sensory encoding stage such that the internal sensory measurement *m* is equal to the input stimulus *s*. But there exists choice variability from measurement *m* to the reported color ($\hat{s}$). Such choice variability does not vary across set size levels. The IL model also assumes a fixed capacity *K*. The response probability is:

$$p(\hat{s} \mid s) \equiv p(\hat{s} \mid m) = \begin{cases} \dfrac{K}{N} VM(\hat{s} \mid s, \kappa_r) + (1 - \dfrac{K}{N}) \dfrac{1}{2\pi}, & K <= N \\ VM(\hat{s} \mid s, \kappa_r), & K > N \end{cases}, \tag{S9}$$

The IL model has two free parameters: choice variability κ_r, and capacity *K*.

Mixture model. The mixture model (MIX) has been used in previous clinical research [6]. Similar to the IL model, the MIX model only assumes the uncertainty from stimulus *s* to the reported color ($\hat{s}$) and a fixed capacity *K*. The difference is that the uncertainty (κ) reflects both sensory noise and choice variability, and thus the uncertainty is set-size dependent (each set size has one κ). The response probability can be written as:

$$p\left(\hat{s} \mid s\right) = \begin{cases} \dfrac{K}{N} VM\left(\hat{s} \mid s, \kappa_{1/3}\right) + \left(1 - \dfrac{K}{N}\right) \dfrac{1}{2\pi}, & K \le N \\ VM\left(s \mid s, \kappa_{1/3}\right), & K > N \end{cases}, \tag{S10}$$

where and denote the uncertainty for set size 1 and 3, respectively. The MIX model has three parameters: uncertainty levels κ_1 and κ_3, and capacity *K*.

Slots-plus-averaging model. The slots-plus-averaging (SA) model was originally proposed in [7] and further elaborated in [1]. Unlike the IL model, the SA model acknowledges the presence of noise in the sensory encoding stage. However, the memory resources are discrete chunks, and a single chunk or multiple chunks can be assigned to one item. For one item, the SA model assumes Eq. S4 still holds as the relationship between the resource assigned to that item and the width of the von Mises distribution:

$$\kappa = \Phi(SJ_s)\ , \tag{S11}$$

where *S* is the number of chunks and J_s is the resource of one chunk. The SA model also assumes a capacity *K*.

When $N > K$, an item should receive either 0 or 1 chunk. Then the allocation should be similar to the IL model. the response distribution should be a mixture of a uniform and a von Mises distributions:

$$p(\hat{s}\,|\,s) = \frac{K}{N}\frac{I_0(\sqrt{\Phi(J_s)^2 + \kappa_r^2 + 2\Phi(J_s)\kappa_r\cos(\hat{s}-s)})}{2\pi I_0(\kappa_r)I_0(\Phi(J_s))} + (1-\frac{K}{N})\frac{1}{2\pi} \quad K < N\ , \tag{S12}$$

When N ≤ K, some items receive either one or more chunks. Assuming that the resource chunks should be assigned as equally as possible across items, the *S* can be calculated as:

$$S = \begin{cases} \left\lfloor \frac{K}{N} \right\rfloor, & \text{with probability } 1\text{-}\frac{K \bmod N}{N} \\ \left\lfloor \frac{K}{N} \right\rfloor + 1, & \text{with probability } \frac{K \bmod N}{N} \end{cases}\ , \tag{S13}$$

where $\lfloor x \rfloor$ represents the *floor* function in Matlab. The corresponding concentration parameter of von Mises distributions can be computed by Eqs. S11&13:

$$\kappa_{low} = \Phi(\left\lfloor \frac{K}{N} \right\rfloor J_s)$$
$$\kappa_{high} = \Phi(\left\lfloor \frac{K}{N} + 1 \right\rfloor J_s) \quad \text{(S14)}$$

The response probability in the SA model can be written as:

$$p(\hat{s} \mid s) = \frac{K \bmod N}{N} \frac{I_0(\sqrt{\kappa_{high}^2 + \kappa_r^2 + 2\kappa_{high}\kappa_r \cos(\hat{s} - s)})}{2\pi I_0(\kappa_r) I_0(\kappa_{high})} + (1 - \frac{K \bmod N}{N}) \frac{I_0(\sqrt{\kappa_{low}^2 + \kappa_r^2 + 2\kappa_{low}\kappa_r \cos(\hat{s} - s)})}{2\pi I_0(\kappa_r) I_0(\kappa_{low})} \quad K > N$$

, (S15)

The SA model has three free parameters: unit resource J_s, choice variability κ_r, and capacity K.

Cosine slots-plus-averaging model. A recent paper [8] suggests that a modified version of the SA model, dubbed cosine slots-plus-average model (cosSA), outperformed the VP model to explain the delay-matching VWM behavior. To enhance the generality of our study, we also followed that work and included this model. Briefly, the cosSA model assumes that the unit memory precision is stimulus-dependent and exhibits a cosine-like periodic fluctuation:

$$J_s = e^{J_m + J_f \cos(8s)}, \quad \text{(S16)}$$

where J_m and J_f describe the fluctuation of unit memory precision (J_s) as a function of stimulus s. We can convert precision J_s to the width of von Mises distributions κ_s according to Eq. S4. According to capacity K, the discrete memory resource allocation is described as Eq. S11-S14. Moreover, the cosSA model also assumes the response bias is periodic:

$$\mu_s = \mu_f \sin(4s), \quad \text{(S17)}$$

where μ_f adjusts the magnitude of the bias. The probability of a response given the stimulus can be described as:

$$p(\hat{s} \mid s) = \begin{cases} \frac{K}{N} VM(\hat{s} \mid s + \mu_s, \kappa_s) + \left(1 - \frac{K}{N}\right)\frac{1}{2\pi}, & K \le N \\ VM(\hat{s} \mid s + \mu_s, \kappa_s), & K > N \end{cases}, \quad \text{(S18)}$$

The cosSA model has four free parameters: J_m, J_f, μ_f and capacity K.

Equal-precision model. The equal-precision (EP) model is very similar to the VP model, except that an equal amount of resources is assigned to every item and in any trial. Namely, the Eq. S2 does not apply to the EP model. In the EP model, the resource assigned to one item declines as a power function (as Eq. S1). Then the resource at each set size level can be converted to the width of the von Mises distribution using (Eq. S4). The response probability is given by:

$$p(\hat{s}\,|\,s;\bar{J}_1,a,\kappa_r)=\frac{I_0\left(\sqrt{\Phi(\bar{J}_1N^{-a})^2+\kappa_r^2+2\Phi(\bar{J}_1N^{-a})\kappa_r\cos(\hat{s}-s)}\right)}{2\pi I_0(\kappa_r)I_0(\Phi(\bar{J}_1N^{-a}))}, \qquad \text{(S19)}$$

where J_1 is the resource when set size is 1 (initial resources). The EP model has three free parameters: initial resources $\bar{J}_1$, decaying exponent a, and choice variability κ_r.

Supplementary Note 2: Intuitive model explanations

Despite the mathematical details provided above, we further provide intuitive explanations for each model and highlight their differences based on cartoon illustrations in Supplementary Fig. 1. Note that all stimuli are 0 because we transformed the reported color to recall errors in each trial.

Item-limit model. In the IL model (Supplementary Fig. 1A), if the capacity K is larger than the set size N (e.g., N=2, K=3, the left panel), all items can enter working memory. The reported color follows a von Mises distribution with the mean as the color of the probed stimulus. If the capacity K is smaller than the set size N (e.g., N=2, K=3, the right panel), a probed stimulus can be stored within memory with probability K/N and out of memory with probability (1-K/N). If the probed stimulus is in memory, the same rule of von Mises distribution applies. If the probed stimulus is out of memory, a subject guesses a color (i.e., with probability 1/2π, the uniform distribution of guessing).

Mixture model. The mixture model (Supplementary Fig. 1B) shares all components with the IL model. The key difference is that the IL model assumes the same von Mises distribution for both set size levels (i.e., same width of the blue and the orange distributions in Supplementary Fig. 1A), while the mixture model uses two von Mises distributions with different widths for the two set size levels (i.e., different widths of the blue and the orange distributions in Supplementary Fig. 1B), to compensate the potential different level uncertainty associated with two set size levels. Thus, the mixture model has one additional free parameter than the IL model.

Slot-plus-averaging and cosine slot-plus-averaging model. The SA model regards memory resources as several discrete chunks (Supplementary Fig. 1C). In the example of Supplementary Fig. 1C, the subject has three (K=3) chunks of resources and the blue cups stand for individual stimulus. If two stimuli are presented (i.e., two cups, set size = 2), the scenario in which the number of resource chunks is larger than the set size, two resource chunks are assigned to one cup and another chunk to the other cup. If the number of resources is smaller than the set size (e.g., four stimuli/cups), one cup will receive no resource, and the subject has to guess if this stimulus/cup is probed. The key difference between the SA model and the three models below is that the SA model assumes discrete resource chunks.

The cosSA model is a modified version of the SA model with three major changes [8]. First, the unit memory precision is stimulus-dependent and follows a periodic function (see Eq. S16 and Fig. S1D). Second, it also includes a response bias that is also stimulus-dependent and periodic (see Eq. S17 above and Fig. S1D). Third, for simplicity it does not include the response variability and only includes one uncertainty (i.g., encoding precision) in the processing.

Equal-precision, variable-precision and variable-precision-with-capacity models. The EP, VP and VPcap models share one core assumption: memory resources are continuous, analogous to the amount of juice in a big mug (Supplementary Fig. 1E). A subject needs to assign the juice (i.e., resources) into different cups (i.e., stimuli). In Supplementary Fig. 1E, the orange cups stand for the mean juice amount an individual cup receives in each set size condition. We can imagine that, given the total amount of juice is fixed, the more cups (i.e., larger set size) the less juice on average each cup will receive. This is reflected by the diminishing average amount of juice as set size increases (also see Eq. S1).

Besides the core assumption of continuous resources, the three models have slightly different specifications (Supplementary Fig. 1F). In Supplementary Fig. 1F, all orange cups stand for the mean juice amount in each set size condition, and the blue cups stand for individual stimulus. The EP model assumes that in each set size condition, each cup receives an identical amount of juice (upper row in Supplementary Fig. 1F). In the VP model, however, each cup receives a variable amount of juice even though their average amount is the same as in the EP model. Using two cups as an example, the average amount of juice might be 10 ml but one cup might have 9 ml and the other one has 11 ml. Whether the amount of juice in each cup varies is the key difference between the EP and the VP models. Moreover, both EP and VP models do not constrain the total number of cups. Therefore, a cup will more or less receive a little bit juice even though there is a large number of cups (middle row). In other words, both the EP and the VP models have no concept of capacity. In contrast, the VPcap model not only inherits the assumption of variable precision and but also constraints the maximal number of cups (i.e., capacity K) that can receive juice. If the total number of cups (i.e., N stimuli) is larger than the capacity K, some cups will receive no juice, and the subject has to guess the color of these stimuli.

Supplementary Note 3: Model fitting and comparisons

Model fitting. The BADS optimization toolbox in MATLAB [9] was used to search the best-fit parameters that maximize the likelihood of response data in all trials. BADS has been shown to outperform other default nonlinear optimization algorithms in MATLAB, especially in the problems where gradients on loss function are not available or hard to compute [9]. We fit all models separately in each participant. To avoid local minima, we repeated the optimization process with 20 different initial seeds that are equally spaced within a lower and an upper bound. Parameters bounds were set to be very broad to avoid bias. The parameters with the maximum likelihood value were used as the best-fit parameters for one subject.

Model comparisons. We compared the performance of all models fitted in this study. Model comparisons were performed for both groups using both Akaike information criterion (AIC) and Bayesian information criterion (BIC) [10,11] metrics (Supplementary Fig. 1). We derived the best model for each subject. Results showed that the VP model outperformed all other models over 84% of subjects in both groups under both AIC and BIC (Supplementary Fig. 2). Particularly, the VP model is the best-fitting model in 51 out of 61 (84%) HC and in 55 out of 60 SZ (92%) under the AIC. Using the BIC, the VP model is the best-fitting model in 52 out of 61 HC (85%) and 54 out of 60 (90%) SZ. These results strongly support the idea that the VP model assuming no fixed capacity better explains the VWM behavior. This result also questions the conventional theory whether capacity acts as a key determinant of limiting VWM performance in SZ.

One might argue that the SA, cosSA, and MIX models were worse than the VP model because AIC and BIC overly penalize the capacity parameter K while this parameter may not substantially improve goodness of fitting because of low set size levels (i.e., 1/3) used here. To exclude this possibility, we further compared the SA, cos SA, and MIX models to the VP model using AIC and BIC metric but without considering the capacity K— that is, we kept the likelihood of the model fitting with K but calculated AIC and BIC without K. In this case, the models fully enjoyed the potential benefits endowed by K in modeling fitting but avoided overly penalizing this additional parameter. Results showed that the VP model was still the best-fitting model in the majority of subjects in both groups and under both metrics (AIC, 51 out of 61 in the HC group and 43 out of 60 in the SZ group; BIC, 52 out of 61 in the HC group and 45 out of 60 in the SZ group).

Supplementary Note 4: Results of other suboptimal models

Fitted parameters of the VPcap model. The VPcap model is a variant of the VP model and incorporates an additional capacity parameter. Estimated parameters in the VPcap model largely replicated the results of the VP model (Supplementary Fig. 3). Again, SZ have larger resource allocation variability than HC (Supplementary Fig. 3B, $t(119) = 3.891$, $p = 1.65 \times 10^{-4}$, $d = 0.707$) and the two groups did not significantly differ in the resource decay function (Supplementary Fig. 3A, initial resources, $t(119) = 0.012$, $p = 0.990$, $d = 0.002$; decaying exponent, $t(119) = 1.142$, $p = 0.256$, $d = 0.208$). We observed a significant larger choice variability in HC (Supplementary Fig. 3C, choice variability, $t(119) = 2.365$, $p = 0.02$, $d = 0.43$). Most importantly, the estimated capacity values of two groups were statistically comparable (Supplementary Fig. 3D, $t(119) = 0.459$, $p = 0.647$, $d = 0.083$).

Comparing capacity of the two groups in suboptimal models. We further investigated the estimated capacity of all subjects in the IL, the SA, the cosSA, the MIX and the VPcap model, the four models having the capacity parameter. We found no significant group difference in capacity measured by all five models (Supplementary Fig. 4, IL model, $t(119) = 1.554$, $p = 0.123$, $d = 0.283$; SA model, $t(119) = 1.03$, $p = 0.306$, $d = 0.187$; cosSA model, $t(119) = 0.235$, $p = 0.815$, $d = 0.043$; MIX model, $t(119) = 0.273$, $p = 0.786$, $d = 0.050$; VPcap model, $t(119) = 0.459$, $p = 0.647$, $d = 0.083$).

Supplementary Note 5: Color perception task

Color perception task. Before the main VWM task, all subjects completed a task to measure their color perception ability. The task is identical to the VWM task except for two modifications. First, only one colored object was shown in the sample array. Second, in the probe array, the colored object appeared again on the screen. A subject needed to choose its color on the color wheel while looking at it. There was 1 block with 50 trials in this task.

Color perception results between HC and SZ. We used the circular standard deviation (CSD) of response errors (the circular distance between the original color and chosen color in a trial) to evaluate the performance in the color task. A significant group difference was found ($t(119) = -2.095$, $p = 0.038$, $d = -0.38$), suggesting in general worse color perception in SZ. But this result might also be explained by potential differences in choice variability (e.g., motor control). To exclude the potential confounding of color perception, we further set CSD from the color perception as a co-variate and repeat all statistical analyses (see below).

Supplementary Note 6: Statistical results with the CSD in the color perception task as a covariate.

VWM performance. We added the CSD in the color perception task as a co-variate to VWM performance comparison of two groups. The repeated-measure ANCOVA (see the main text for details of variables) results again showed a worse VWM performance at higher set size level ($F(1,119) = 100.676$, $p < 0.001$, partial $\eta^2 = 0.46$). The group was also significant ($F(1,119) = 8.902$, $p = 0.003$, partial $\eta^2 = 0.070$), indicating that HC's performance was better than SZ's. The interaction between set size and group was not significant ($F(1,119) = 0.324$, $p = 0.570$, partial $\eta^2 = 0.003$). Also, the color perception ability had no influence on VWM performance ($F(1,119) = 0.285$, $p = 0.595$, partial $\eta^2 = 0.002$). These results replicated the results from the main text.

Fitted parameters of the VP model. Univariate general linear models were used for comparing fitted parameters between the two groups. We regressed out the factor of color perception by setting. Same as results in the main text (Fig. 5), comparable resource decay functions (Fig. 5A, initial resources, $F(1,119) = 0.376$, $p = 0.541$, partial $\eta^2 = 0.003$; decaying exponent, $F(1,119) = 0.573$, $p = 0.451$, partial $\eta^2 = 0.005$) and choice variability (Fig. 5C, $F(1,119) = 1.702$, $p = 0.195$, partial $\eta^2 = 0.014$) between SZ and HC were found in this analysis. And SZ showed larger variability in allocating resources (resource allocation variability, $F(1,119) = 15.112$, $p < 0.001$, partial $\eta^2 = 0.114$).

Fitted parameters of the VPcap model. The two groups did not show significant differences in the resource decay function (initial resources, $F(1,119) = 0.557$, $p = 0.457$, partial $\eta^2 = 0.005$; decaying exponent $F(1,119) = 2.097$, $p = 0.150$, partial $\eta^2 = 0.017$). SZ had larger resource allocation variability ($F(1,119) = 11.490$, $p = 0.001$, partial $\eta^2 = 0.089$) and smaller choice variability $F(1,119) = 5.616$, $p = 0.019$, partial $\eta^2 = 0.045$) than

HC. The estimated capacity values of two groups were statistically comparable (Supplementary Fig. 2D, $F(1,119) = 0.175$, $p = 0.667$, partial $\eta^2 = 0.001$).

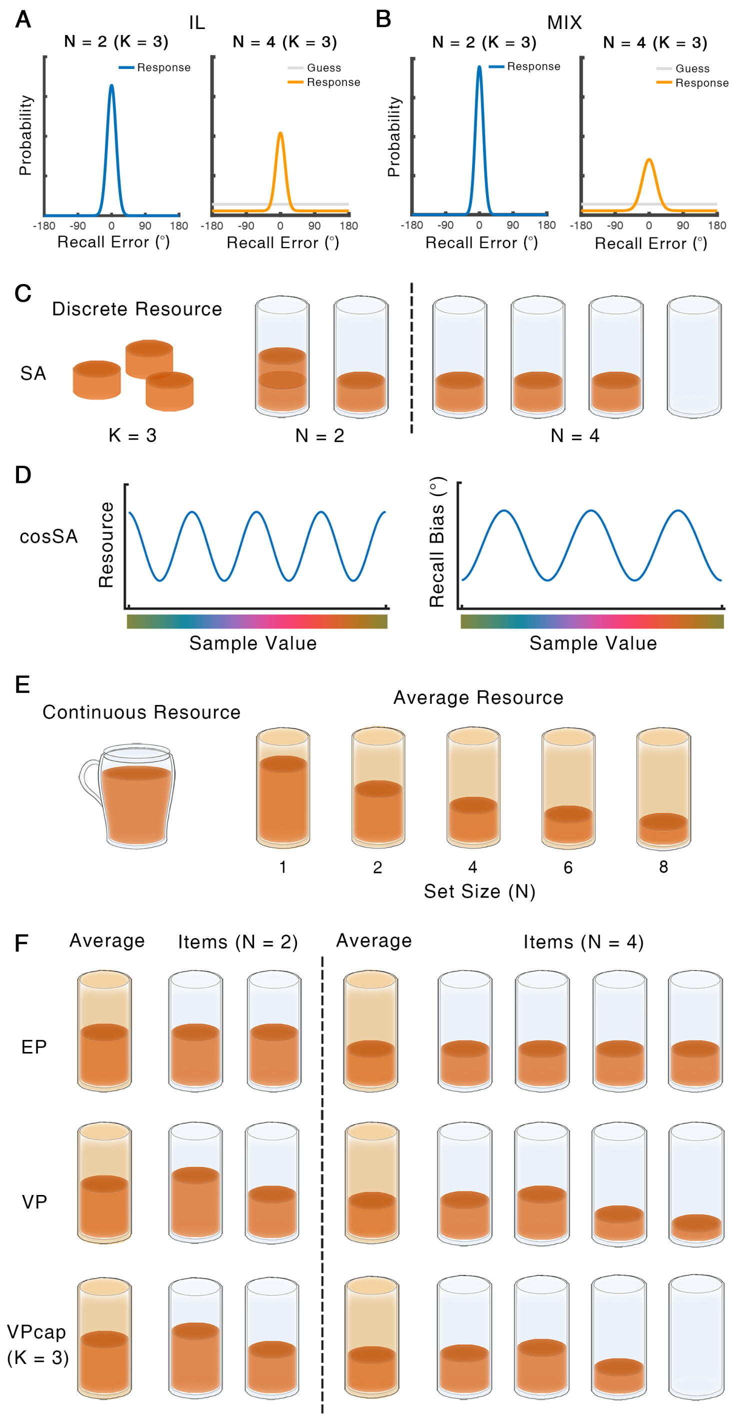

Supplementary Figure 1. Cartoon illustration of all computational models considered in this study. This figure aims to aid an intuitive understanding of the models. Detailed model explanation to Supplementary Note 2. ***A***. item-limit model; ***B***. MIX model; ***C***. the principle of discrete slots and the SA model; ***D***. cosSA model; ***E***. the principle of continuous resources; ***F***, EP, VP, and VPcap models.

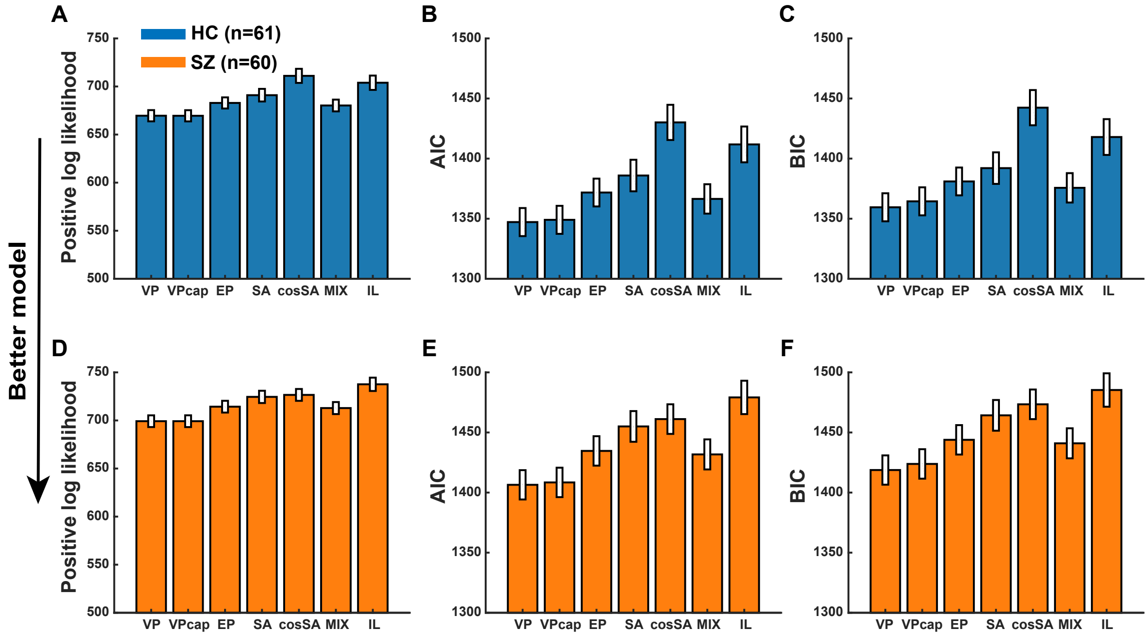

Supplementary Figure 2. Positive log-likelihood (panels A, D), AIC (panels B, E) and BIC (panels C, F) values for all models. Note that here we display the positive log-likelihood values to help visually compare models since maximum negative log-likelihood values are equivalent to minimum positive log-likelihood values. As such, in all panels a lower y-axis value indicates a better model. The upper (panels A-C) and lower (panels D-F) rows depict the model comparison results for HC and SZ respectively. The best-fitting model is the VP model for both groups (also see Fig. 3 in the main text).

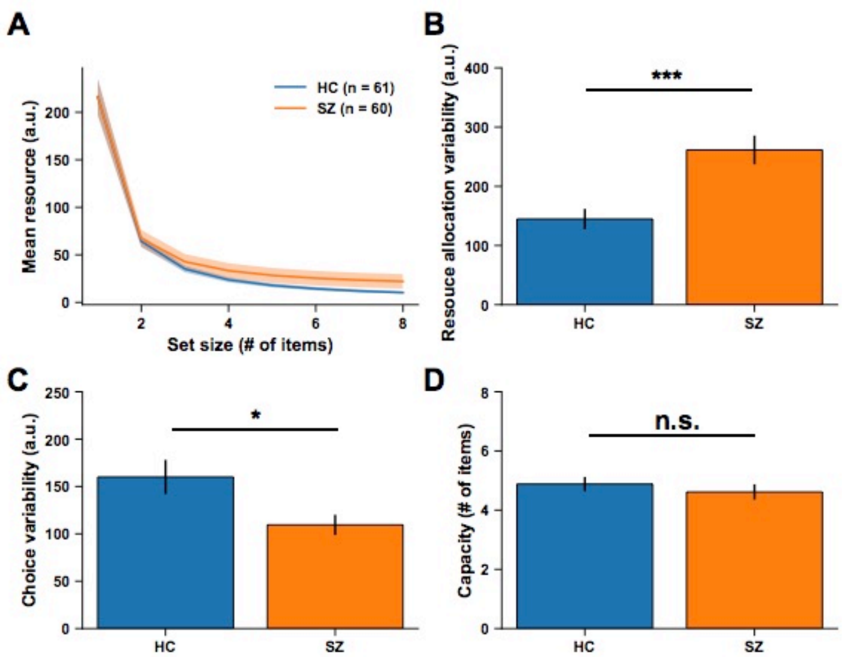

Supplementary Figure 3. Fitted parameters (panel A: resource decay functions; panel B: resource allocation variability; panel C: choice variability; panel D: capacity) of the VPcap model. The results replicate the results in Fig. 4. Furthermore, this model estimates capacity in individual subjects and the result show that the two groups have a comparable capacity (panel D). All error bars are ± SEM across subjects. Other figure captions are the same as in Fig. 4 in the main text. Significance symbol conventions are *:p < 0.05; ***: p < 0.001; n.s.: non-significant.

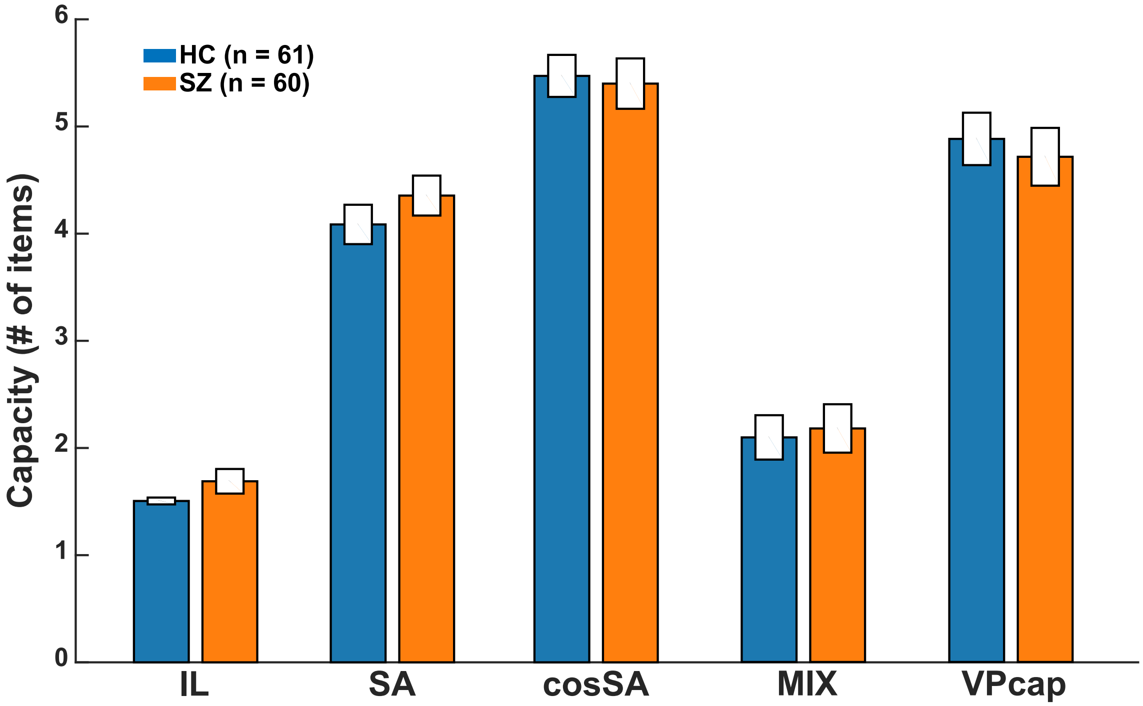

Supplementary Figure 4. The capacity of the two groups measured by five suboptimal models. None of the five models reveal the significant group differences in capacity. These results directly challenge the conventional decreased-capacity account of SZ. All error bars are ± SEM across subjects.

References

1. van den Berg, R., Shin, H., Chou, W.-C., George, R. & Ma, W. J. Variability in encoding precision accounts for visual short-term memory limitations. *Proc. Natl. Acad. Sci.* **109,** 8780–8785 (2012).
2. van den Berg, R., Awh, E. & Ma, W. J. Factorial comparison of working memory models. *Psychol. Rev.* **121,** 124–149 (2014).
3. Bays, P. M. & Husain, M. Dynamic Shifts of Limited Working Memory Resources in Human Vision. *Science (80-.).* **321,** 851–854 (2008).
4. Bays, P. M., Catalao, R. F. G. & Husain, M. The precision of visual working memory is set by allocation of a shared resource. *J. Vis.* **9,** 7.1-11 (2009).
5. Ma, W. J., Beck, J. M., Latham, P. E. & Pouget, A. Bayesian inference with probabilistic population codes. *Nat. Neurosci.* **9,** 1432–1438 (2006).
6. Gold, J. M. *et al.* Reduced Capacity but Spared Precision and Maintenance of Working Memory Representations in Schizophrenia. *Arch. Gen. Psychiatry* **67,** 570–577 (2010).
7. Zhang, W. & Luck, S. J. Discrete fixed-resolution representations in visual working memory. *Nature* **453,** 233–235 (2008).
8. Pratte, M. S., Park, Y. E., Rademaker, R. L. & Tong, F. Accounting for stimulus-specific variation in precision reveals a discrete capacity limit in visual working memory. *J. Exp. Psychol. Hum. Percept. Perform.* **43,** 6–17 (2017).
9. Acerbi, L. & Ma, W. J. Practical Bayesian Optimization for Model Fitting with Bayesian Adaptive Direct Search. in *Advances in Neural Information Processing Systems 30* 1836–1846 (2017). doi:https://doi.org/10.1101/150052
10. Wit, E., van den Heuvel, E. & Romeijn, J. W. 'All models are wrong. ': An introduction to model uncertainty. *Stat. Neerl.* **66,** 217–236 (2012).
11. Burnham, K. P. & Anderson, D. R. *Model Selection and Multimodel Inference: A Practical Information-Theoretic Approach*. *Ecological Modelling* **172,** (Springer-Verlag, 2002).